OAK RIDGE NATIONAL LABORATORY
MANAGED BY UT-BATTELLE FOR THE DEPARTMENT OF ENERGY

ORNL/TM-2012/221

Performance Evaluation of HYCOM-GOM for Hydrokinetic Resource Assessment in the Florida Strait

June 2012

Prepared by

Vincent S. Neary, Ph.D., P.E., Budi Gunawan, Ph.D., Albert Ryou

UT-BATTELLE

ORNL/TM-2011/221

Environmental Science Division

Performance Evaluation of HYCOM-GOM for Hydrokinetic Resource Assessment in the Florida Strait

Vincent S. Neary, Ph.D., P.E.
Budi Gunawan, Ph.D.
Albert Ryou

Date Published: June 22, 2012

Prepared by
OAK RIDGE NATIONAL LABORATORY
Oak Ridge, Tennessee 37831-6283
managed by
UT-BATTELLE, LLC
for the
U.S. DEPARTMENT OF ENERGY
under contract DE-AC05-00OR22725

EXECUTIVE SUMMARY

The U.S. Department of Energy (DoE) is assessing and mapping the potential off-shore ocean current hydrokinetic energy resources along the U.S. coastline, excluding tidal currents, to facilitate market penetration of water power technologies. This resource assessment includes information on the temporal and three-dimensional spatial distribution of the daily averaged power density, and the overall theoretical hydrokinetic energy production, based on modeled historical simulations spanning a 7-year period of record using HYCOM-GOM, an ocean current observation assimilation model that generates a spatially distributed three-dimensional representation of daily averaged horizontal current magnitude and direction time series from which power density time series and their statistics can be derived. Our aim is to examine the deviation of HYCOM-GOM outputs from the HYCOM-GLOBAL model, and those based on three independent observation sources: NOAA's submarine cable transport data, Florida Atlantic University's (FAU) ADCP data at a high power density location, and the Southeast Coastal Ocean Observing Regional Association's (SECOORA) HF radar data in the high power density region of the Florida Strait. Comparisons with these three independent observation sets, and HYCOM-GLOBAL outputs, indicate discrepancies with HYCOM model outputs, but overall that the HYCOM-GOM model can provide a *best-practical* assessment of the ocean current hydrokinetic resource in high power density regions like the Florida Strait, but that there may be ways to improve predictions through improved data assimilation and model forcing for periods when predictions of temporal variation of transport are less accurate than other periods, and by inclusion of additional independent observational data sources, e.g. ADCP measurements.

INTRODUCTION

The U.S. Department of Energy (DoE) is assessing and mapping the potential off-shore ocean current hydrokinetic energy resources along the U.S. coastline, excluding tidal currents, to facilitate market penetration of water power technologies. This resource assessment includes information on the temporal and three-dimensional spatial distribution of the daily averaged power density, and the overall theoretical hydrokinetic energy production, based on a modeled historical simulation spanning 2004 to 2010.

The main model employed for this resource assessment is HYCOM, an ocean current data assimilation model that combines physical ocean current data from a wide variety of spatial coverage and temporal scales at various resolutions. HYCOM simulations of historical ocean currents over a given period of record generate a spatially distributed three-dimensional representation of daily averaged horizontal current magnitude and direction time series from which power density time series and their statistics can be derived (Haliwell 2002, Hanson et al. 2011, Duerr and Dhanak 2012).

We evaluate the quality of outputs from the Gulf of Mexico HYCOM model (HYCOM-GOM), which provides daily spatial averaged values of current magnitude and direction within 4 km x 4 km grid cells uniformly distributed in the Florida Strait, and consisting of 40 layers nonuniformly distributed in the vertical water column. The vertical height of the 4 km x 4 km cells within each column varies from 5m near the surface to values of 10 m, 25 m, 50 m, 100 m, 250 m and 500 m with increasing depth. A similar study in the Florida Strait reported the model performance of the Global HYCOM model (HYCOM-GLOBAL), based on comparison with NOAA submerged telephone cable measurements of transport (flow), which has a coarser computational mesh consisting of 7 km x 7 km grid cells, and 33 vertical layers, with a similar distribution of vertical height as HYCOM-GOM (Duerr and Dhanak 2012).

Our aim is to quantify deviations of HYCOM-GOM outputs from those derived from independent observations using standard performance plots and metrics. Agreement between HYCOM outputs and those derived from independent observations would indicate that the HYCOM-GOM model simulations produce valid representations of spatially and temporally varying power density, and that the theoretical energy rate available (power) can be assessed for a given region. However, what constitutes good agreement is oftentimes subjective and depends on a number of factors, including model performance goals, the grid resolution, grid dependency, and the quality, and temporal and spatial resolution of the independent observations.

As the purpose of the ocean current resource assessment is to provide a *best-practical* model prediction of the mean annual energy production and the spatial distribution of power density for different ocean current regions in the US, our model performance evaluation emphasizes the ability of the model to predict temporal mean values of power density, rather than its temporal variations, especially at depths that are considered practical for current energy extraction. Our model performance evaluation assumes independent observations sources (*measurements*) are true values, but these observations are also subject to errors, and often only approximately correspond to model outputs, or measurements using other

techniques. The accuracy of HF radar velocity measurements, for example, has been examined by comparison with ADCP measurements in a number of studies (Holbrook and Frisch, 1981; Matthews et al., 1988; Chapman et al., 1997; Graber et al., 1997; Nadai et al., 1997, Yoshikawa et al. 2005, Shay et al. 2008). Differences between near surface velocity measurements by HF radar and ADCP are due to instrument noise, collocation and concurrence differences, and beam pattern departure (Shay et al. 2008, Graber et al. 1997). The root mean square difference is ~15 cm/s when comparing radar measurements of velocity to those by ADCP. However, measurements using these two different techniques are not spatially coincident. HF radar measurements are averaged over an area of ~a few km^2 near the surface (~1 m), while ADCP measurements are averaged over ~0.1 m^2 (effectively a point) and at depths ≥several meters. Similarly point velocity measurements using an ADCP are not spatially coincident to measurements spatially averaged over the HYCOM model grid cells.

METHODS

We selected the high power density region of the Florida Strait, delineated by the white box in Fig. 1, as our study site for several reasons. First, it represents the dominant ocean current resource in the United States, with the largest power densities in the US, and closest proximity to the coast compared to all other US ocean current resource regions. Second, the Florida Current has been extensively studied over three decades, and particularly for hydrokinetic energy resource assessment (Arx et al. 1974, Stewart 1974, Raye 2002, Hanson et al. 2011). Finally, a variety of independent observational data sources are available in the Florida Strait, including the NOAA submerged telephone cable measurements, ADCP measurements by Florida Atlantic University (FAU), and HF radar measurements available through the Southeast Coastal Ocean Observing Regional Association (SECOORA) .

Our model performance evaluation methodology is similar to that described by Stewart and Neary (2011) for the tidal resource assessment model validation. First, the HYCOM power density time series spanning 2004 to 2010 are processed to be spatially and temporally concurrent with the independent observation data sources. The HYCOM simulated time series of the daily averaged current magnitude and direction are available for downloaded at the website http://hycom.org/. The current magnitude time series in each 4 km x 4 km grid cell is used to calculate the daily averaged power density time series as detailed by others (e.g. Duerr and Dhanak 2012, Defne et al. 2012). The bulk flow time series over this POR is calculated by integrating the northern component of the current magnitude over the cross section area, which is normal to the submarine telephone cable.

Independent data sources for calculating comparable HYCOM outputs include seven coincidental years of underwater flow time series data derived from a submarine telephone cable, corrected for geomagnetic variations and with the tidal signal removed (Larsen 1991, Baringer and Larsen 2001, Baringer and Meinen 2010, Meinen et al. 2010), two coincidental years of current magnitude time series data derived from acoustic Doppler current profiler (ADCP) measurements at a high power density location (26.07167N-79.84167W) from 26

February 2009 to 25 March 2010 (Duerr and Dhanak 2012), and two coincidental years of daily averaged current magnitude (surface only) time series derived from high frequency (HF) long-range SeaSondes (SS) radar measurements described by Shay et al. (2008). These HF radar measurements average current magnitude and direction within 6 km x 6 km grid cells evenly distributed in the high power density region of the Florida Strait, which is delineated by the white box in Fig. 1, from April 2008 to May 2010 (Personal communication, Paul Reuter, 11 April, 2012). Comparing HYCOM outputs with those derived from three independent data sources allows a rigorous and comprehensive evaluation of the HYCOM model because each data source has different spatial and temporal coverages. While the submarine cable data set does not allow calculation of horizontal current and power density for comparison with HYCOM, it is fundamentally important to check that HYCOM can reproduce bulk flow variations in the Florida Strait, before looking at higher order flow field properties. The moored ADCP data provides current measurements only at a single point in the Strait, but it is the only data source that measures along a vertical water column; thereby allowing assessment of HYCOM's ability to predict the vertical variation of ocean currents. HF radar provides near real-time surface current measurements over large areas up to 259 square kilometers. While limited to surface currents only, these observations, unlike point ADCP measurements, provide a means to evaluate how well ocean models predict the horizontal spatial distribution of ocean current magnitudes and directions.

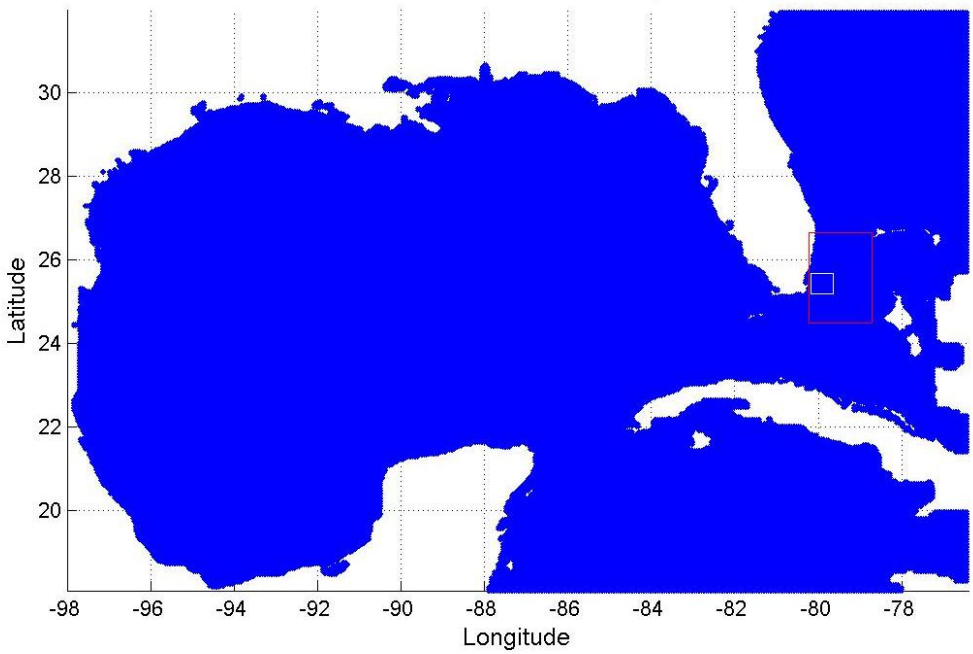

Figure 1. Plot of HYCOM-GOM data availability (blue), study region, the Florida Strait (red box), and high power density region in Florida Strait (white box).

Daily averaged transport (flow) time series from the submarine cable were downloaded from the NOAA website http://www.aoml.noaa.gov/phod/floridacurrent/data_access.php and required no post-processing to make spatially and temporally coincidental comparisons with daily averaged flow time series calculated using HYCOM. The locations of the HYCOM model cross-sections for HYCOM-GLOBAL and GOM HYCOM relative to the submarine cable are shown in Fig. 2. The HYCOM model sections are aligned with the east-west axis and do not align exactly with the cable. The HYCOM-GLOBAL and GOM HYCOM section lines are not exactly aligned because these models have different grids that do not align. The HYCOM-GLOBAL section line is located at latitude 26.5906N, while the GOM line is located at latitude 26.6264N.

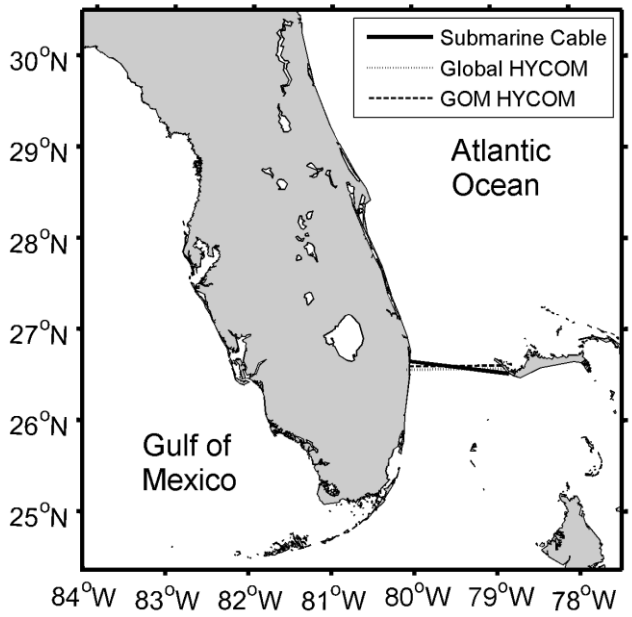

Figure 2. Location of NOAA submarine cable and HYCOM model flow sections used to calculate transport.

Moored ADCP horizontal current magnitude time series data was used to calculate the power density and daily averaged for direct comparison with those derived from HYCOM predicted daily averaged current magnitude. The ADCP derived power density time series were compared to HYCOM-GLOBAL and HYCOM-GOM derived time series of this variable at six depths, 60, 70, 80, 90, 150, 200 and 250 meters, along the vertical water column located at the closest HYCOM-GLOBAL and HYCOM-GOM grid cell centers, located at coordinate location 26.090N, -79.840W, to the ADCP's coordinate location, 26.07167N, -79.84167W. The ADCP site at 60 m depth was used to provide inflow characteristics for designing DOE's reference model ocean current turbine (Personal communication, Michael Lawson, 14 June 2012).

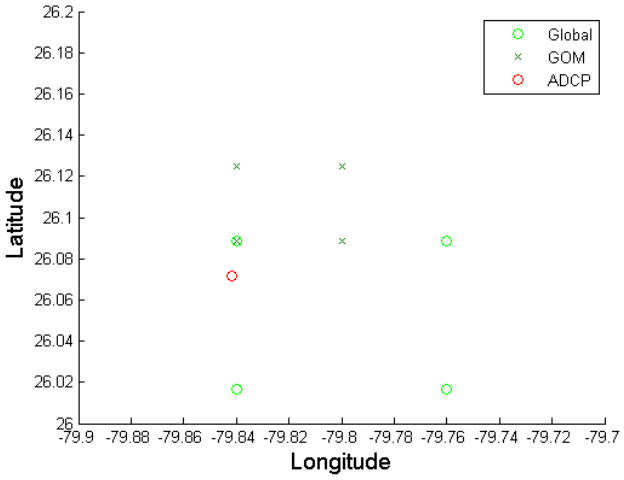

Figure 3. Location of FAU ADCP profile and Global and GOM HYCOM model profiles.

The surface current magnitude time series from HF radar measurements, as for the ADCP data, was used to calculate the power density, daily averaged for direct comparison with those derived from HYCOM-GOM surface current magnitude, and spatially averaged over a 30 km x 30 km area consisting of twenty-five HF radar cells, which, as shown in Fig. 4, overlay best with a 28 km x 28 km area consisting of forty-nine HYCOM-GOM cells centered at 25.5118N,-79.8805W.

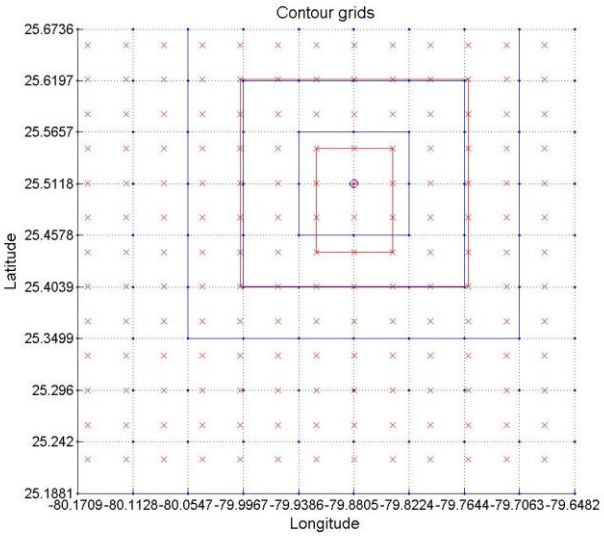

Figure 4. Overlay of HYCOM-GOM grid points (red x) and HF radar grid points (blue dots) in high power density region of Florida Strait. Grid points delineating a 28 km x 28 km area and 30 km x 30 km area in HF radar align best and were therefore used for subsequent time series analysis.

Differences between *predicted* (HYCOM-GOM) and *measured* (observation data) power density time series were qualitatively and quantitatively evaluated using standard model performance plots and metrics commonly used in the literature (e.g. Neary et al. 2004, Stewart and Neary 2011). In addition, HYCOM-GOM and HYCOM-GLOBAL outputs for transport and vertical profiles of horizontal current and power density were visually compared in plots. Performance plots include: scatter plots (predicted vs. measured daily values of power density) from which performance metrics amplitude ratio AR, Intercept, and correlation coefficient R^2 are calculated; frequency histograms, which allow qualitative comparison of mean values, data spread, and the distribution shape; and cumulative frequency histograms, which are useful for comparing how often power densities exceed a specific value of interest. Performance metrics (summary statistics) are calculated for the HYCOM-GOM model predictions only, and include direct comparisons of the mean, minimum and maximum values of predictions and measurements, root-mean-square difference (RMSD), and bias difference.

RESULTS

Submarine Cable Data

Plots comparing measured and predicted transport (flow) time series, paired values, and frequency histograms are shown in Figs. 5-9. Comparisons of HYCOM-GOM and HYCOM-GLOBAL predicted vs. measured daily transport are shown in Figs. 5 and 6. HYCOM-GOM predictions agree better with measurements than those by HYCOM-GLOBAL. Over the entire POR the mean transport predicted by HYCOM-GOM (31.7 Sv) matches closely with that measured by cable (31.4 Sv). The RMSD is only 10%, and bias difference is only 1%. However, the HYCOM-GOM transport time series exhibits less variance than cable measurements and HYCOM-GLOBAL, and the most pronounced measured peaks and nadirs are not predicted by HYCOM-GOM.

Table 1 summarizes the main performance metrics observed in the time series and performance plots for HYCOM-GOM. The maximum and minimum transport values observed for the cable data in the last quarter of 2008, 40.7 Sv and 18.5 Sv, are close to those predicted by HYCOM, 37.3 Sv and 23.8 Sv, but occur at different times in the POR. Largest differences between predicted and measured daily transport are observed in the last quarter of 2008, which falls in the POR of Deurr and Dhanak (2012). Poor performance for this period is examined further by comparing monthly averaged transport derived from HYCOM-GOM simulations, with HYCOM-GLOBAL and cable data. As with the daily averaged transport comparison, the mean monthly averaged transport predicted by HYCOM-GOM (31.9 Sv) agrees better with the mean value based on cable data (31.7 Sv) than that predicted by HYCOM-GLOBAL (28.4 Sv). However, monthly averaged transport from HYCOM-GLOBAL, while exhibiting a significant low bias difference, follows the measured trends much better for some periods than those from HYCOM-GOM. As HYCOM-GOM is a higher resolution model, this result is counterintuitive, and requires further examination of the assimilation methods used in each model.

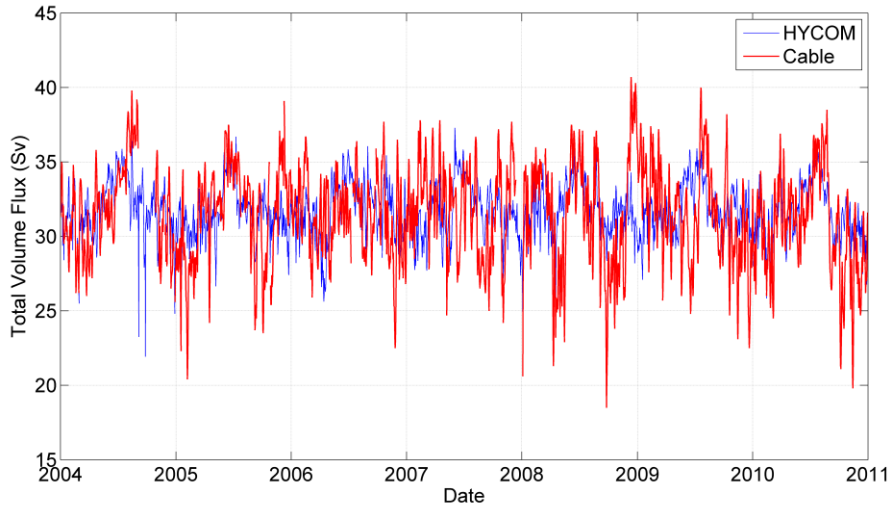

Figure 5. Comparison of Florida Strait transport (flow) variation with time derived from HYCOM-GOM simulations and submarine telephone cable data (2004-2010). Units in Sverdrups, 1 Sv=10^6 m^3/s.

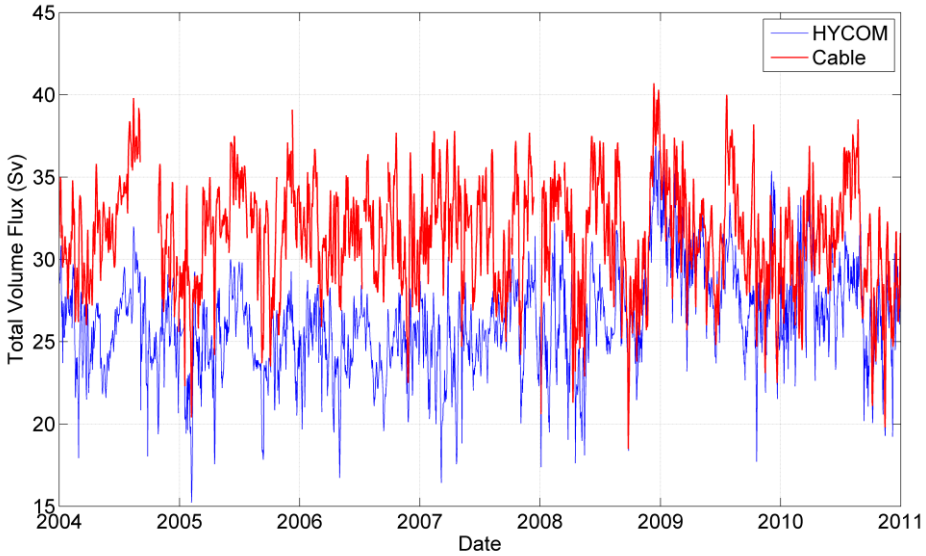

Figure 6. Comparison of Florida Strait transport (flow) variation with time derived from Global HYCOM simulations and submarine telephone cable data (2004-2010). Units in Sverdrups, 1 Sv=10^6 m^3/s.

Table 1. Performance metrics, HYCOM-GOM vs. Submarine cable derived Florida Strait transport (flow)

Time Interval	Flow ($x10^6$ m^3/s)						AR	Intcpt	R^2	RMSD (%)	Bias (%)
	Mean		Min		Max						
	Msrd	Pred	Msrd	Pred	Msrd	Pred					
Daily	31.36	31.68	18.50	23.81	40.70	37.29	0.2027	25.32	0.1345	9.976	0.9963

Daily transport values derived from HYCOM-GOM and cable data are positively correlated, as shown in the scatter plot (Fig. 7), but exhibit large scatter about the line of perfect agreement and the best-fit line. The large scatter is reflected in the low correlation coefficient R^2=0.13. The best fit line indicates that HYCOM has a tendency to underestimate transport when it is above the mean value of transport, 32 Sv (See Fig. 4a), and overestimate transport when it is below this value.

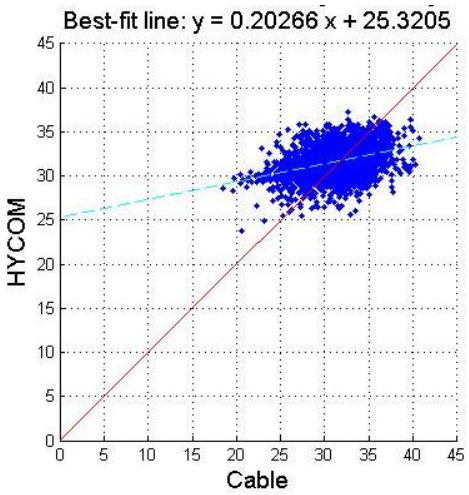

Figure 7. Comparison of Florida Strait daily transport (flow) derived from HYCOM-GOM simulations and submarine telephone cable data. Units in Sverdrups, 1 Sv=10^6 m^3/s.

HYCOM-GOM model performance is examined further by comparing plots of frequency histograms (Fig. 8), and cumulative frequency histograms (Fig. 9) of daily averaged transport derived by HYCOM-GOM and cable data. Both predicted and measured daily averaged transport values are normally distributed about their mean values, which, as mentioned, are in close agreement. The measured transport exhibits greater variance about its mean than the predicted transport, which was also observed in the time series plots. However, the right limbs of the frequency histograms compare better than the left, indicating that HYCOM-GOM matches the frequency of high transport measurements better than low ones. The shapes of

the cumulative frequency histograms, shown in Fig. 9, also compare well. Both indicate that the mean transport (32 Sv) is equaled or exceeded 40% of the time. Like the scatter plot (Fig. 5), Fig. 9 shows that HYCOM GOM has a tendency to overestimate transport, when it is below 32 Sv and underestimate transport, when it is above this value.

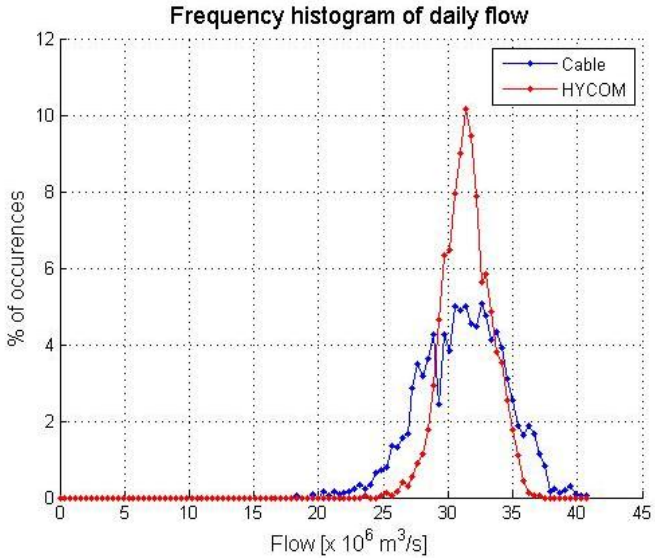

Figure 8. Comparison of frequency histograms for Florida Strait daily transport (flow) derived from HYCOM-GOM simulations and submarine telephone cable data. Units in Sverdrups, 1 Sv=10^6 m^3/s.

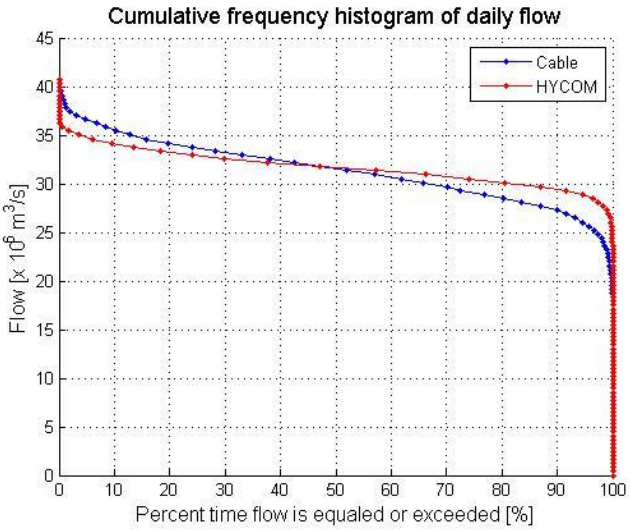

Figure 9. Comparison of cumulative frequency histograms for Florida Strait daily transport (flow) derived from HYCOM-GOM simulations and submarine telephone cable data. Units in Sverdrups, 1 Sv=10^6 m^3/s.

ADCP Data

The *predicted* and ADCP *measured* velocity profiles, including mean, minimum and maximum over the 391 day POR, are compared in Figs. 10 and 11 for the GOM and the Global model results. With the exception of the minimum velocities near the surface, the GOM model predicts larger velocities than those measured. The GOM overbias of mean velocity is most pronounced at depths of 80 m to 200 m, but at 60 m, the reference model depth, predictions agree well with measurements. In contrast, GLOBAL predictions of mean and maximum velocity show a significant underbias at depths up to 200m. GLOBAL underbias of mean and maximum velocities is most pronounced at depths up to 100 m, and particularly at the reference model depth of 60m. These same discrepancies are observed in Figs. 12 and 13, which compare power density profiles predicted using GLOBAL and GOM models with those derived by ADCP measurements.

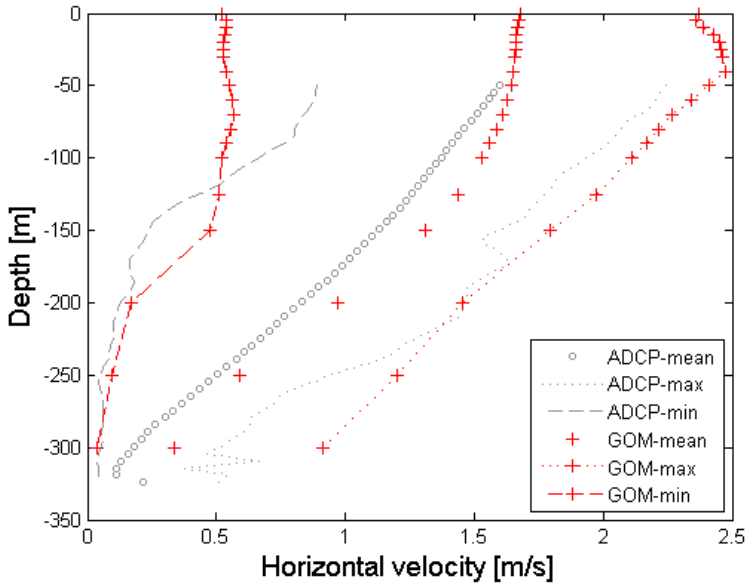

Figure 10. Comparison of daily-averaged current profile averaged over POR (391 days) derived from HYCOM-GOM simulations and FAU ADCP data at 26.07167N-79.84167W.

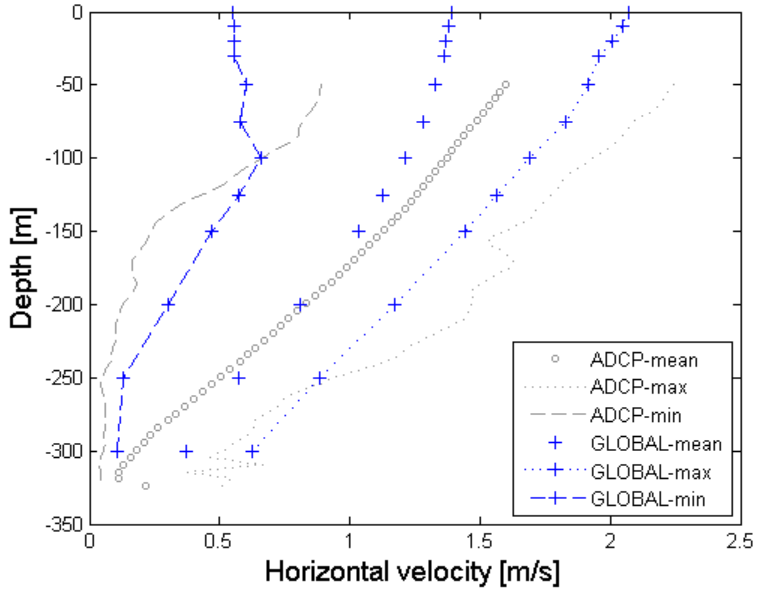

Figure 11. Comparison of daily-averaged current profile averaged over POR (391 days) derived from HYCOM-GLOBAL simulations and FAU ADCP data at 26.07167N-79.84167W.

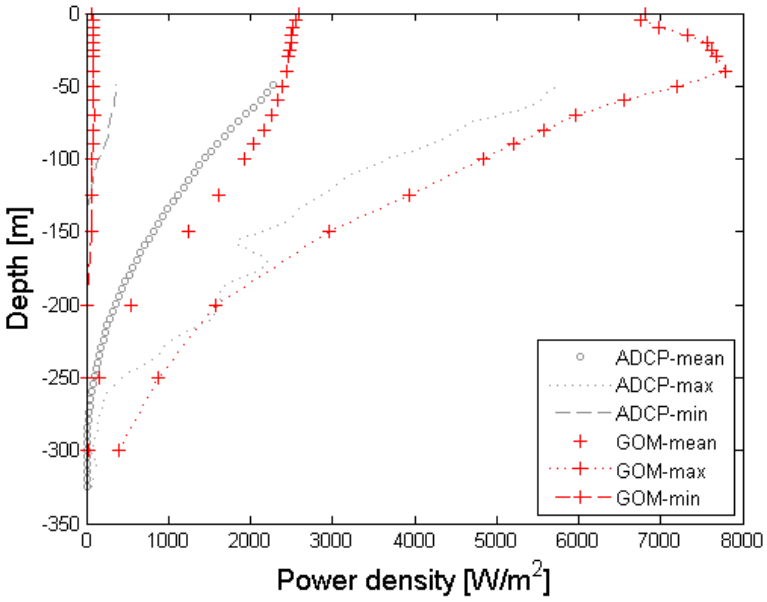

Figure 12. Comparison of daily-averaged power density profile averaged over POR (391 days) derived from HYCOM-GOM simulations and FAU ADCP data at 26.07167N-79.84167W.

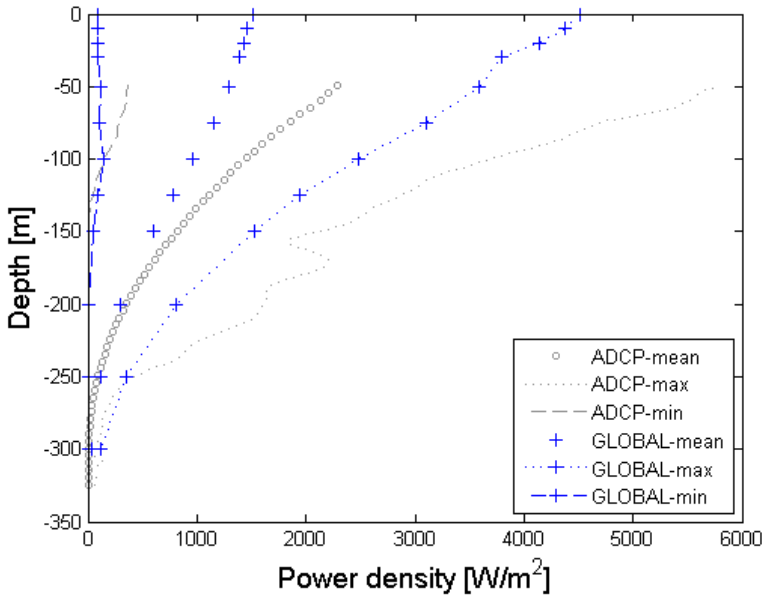

Figure 13. Comparison of daily-averaged power density profile averaged over POR (391 days) derived from HYCOM-GLOBAL simulations and FAU ADCP data at 26.07167N-79.84167W.

Table 2 summarizes the main performance metrics observed in the profile and performance plots for the HYCOM-GOM model only. The agreement between the mean and the maximum power density at the reference model depth of 60 m is quite good. The RMSD and bias difference increase with depth, ranging from 47.7% to 233%, and 8.57% to 95.3%. As velocity and power density decrease with depth, this suggests that HYCOM-GOM more accurately predicts power densities exceeding 1000 W/m^2, which are desirable for hydrokinetic energy conversion.

Table 2. Performance metrics, HYCOM-GOM vs. ADV derived power density.

Depth (m)	Time Interval	Power Density (W/m^2)						AR	Intcpt	R^2	RMSD (%)	Bias (%)
		Mean		Min		Max						
		Msrd	Pred	Msrd	Pred	Msrd	Pred					
60	Daily	2149	2333	350.9	90.99	5567	6556	0.42	1431	0.28	47.68	8.57
70	Daily	1967	2251	311.4	94.79	5127	5965	0.42	1430	0.27	50.94	14.44
80	Daily	1784	2158	272.2	86.93	4583	5575	0.42	1407	0.25	54.63	20.99
90	Daily	1617	2046	239.2	79.73	4241	5213	0.43	1355	0.24	57.81	26.54
150	Daily	774.7	1250	6.860	55.44	1867	2962	0.45	900.5	0.10	94.64	61.40
200	Daily	370.6	545.6	2.470	2.430	1524	1578	0.12	499.3	0.01	113.3	47.22
250	Daily	78.18	152.7	0.140	0.420	381.8	882.3	-0.01	152.4	0.00	233.4	95.28

Daily power density values derived from HYCOM-GOM predictions and ADCP measurements at 60 m depth are positively correlated, as shown in the scatter plot (Fig. 14), but exhibit large scatter about the line of perfect agreement and the best-fit line. The large scatter is reflected in the low correlation coefficient R^2=0.28. The best fit line indicates that HYCOM-GOM has a tendency to underestimate power density when it is above 2500 W/m^2, near the mean value of 2149 W/m^2, and overestimate power density when it is below this value.

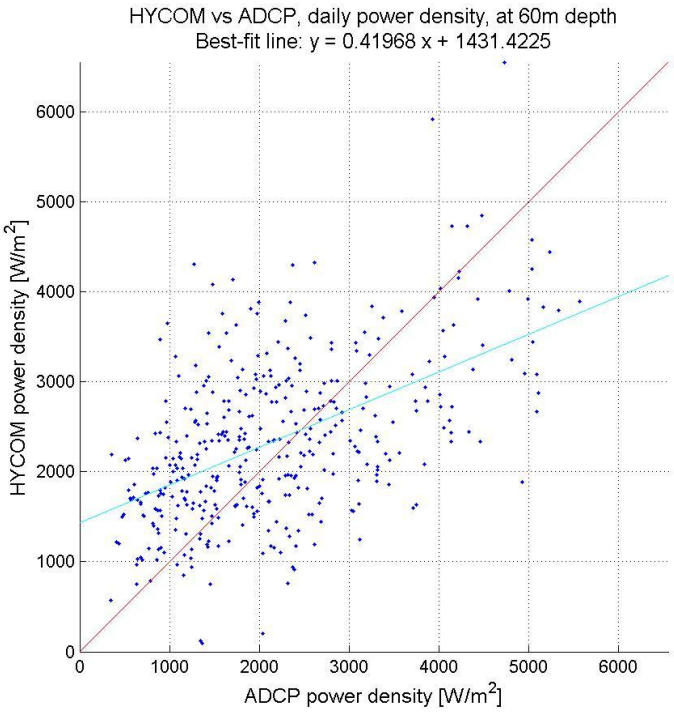

Figure 14. Comparison of power density derived from HYCOM-GOM simulations and ADCP data.

Plots of frequency histograms and cumulative frequency histograms of daily averaged power density predicted by HYCOM-GOM are compared with those derived by ADCP data at 60 m depth in Figs. 15 and 16. Both frequency histograms are nearly Gaussian and match well; as do the cumulative frequency histograms. Both indicate that the mean power density (2149 W/m^2) is equaled or exceeded approximately 40% of the time. The cumulative frequency histogram (Fig. 16) shows that GOM has a tendency to overestimate power density, when it is below 3000 W/m^2, which is equaled or exceeded 20% of the time, and underestimate power density when it is above this value.

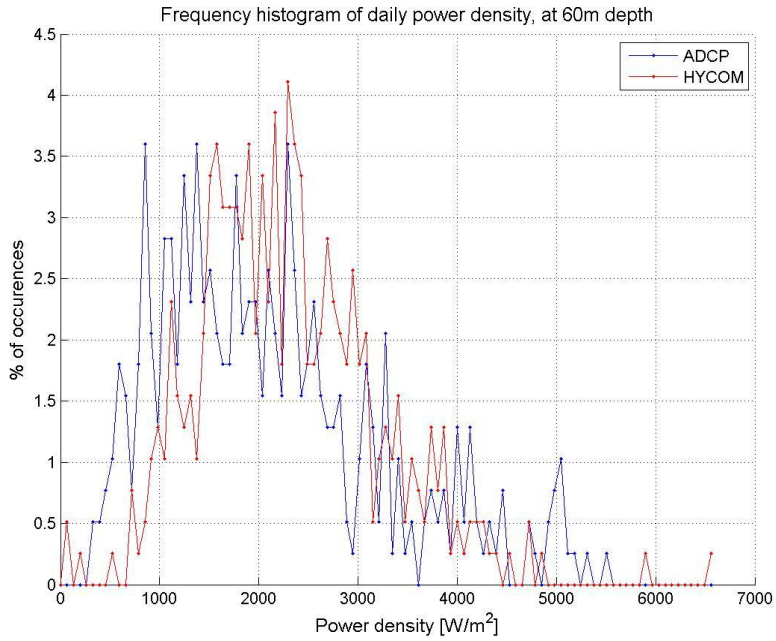

Figure 15. Comparison of frequency histograms of power density derived from HYCOM-GOM simulations and ADCP data.

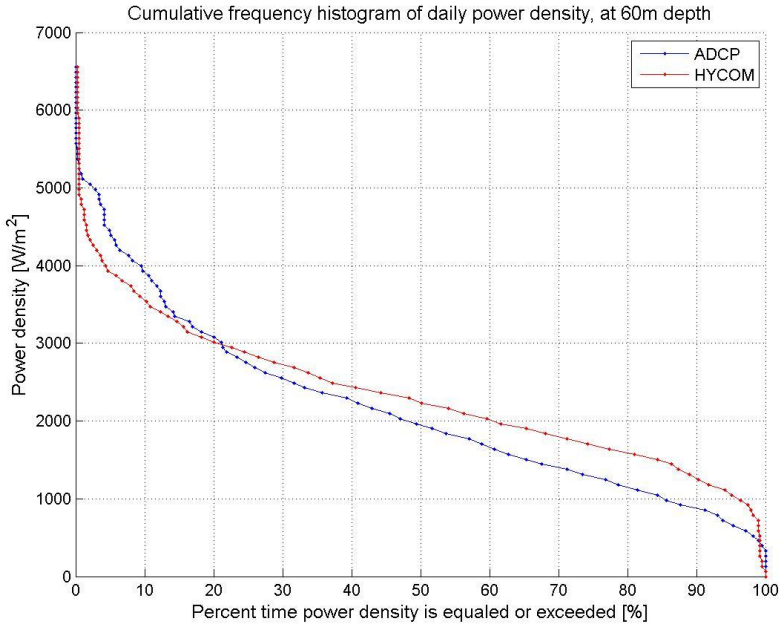

Figure 16. Comparison of cumulative frequency histograms of power density derived from HYCOM-GOM simulations and ADCP data.

HF Radar Data

HF radar measured and predicted power density time series, paired power density values, and power density frequency histograms are shown in Figs. 17-20. Table 3 summarizes the main performance metrics observed in the time series and performance plots. The HYCOM-GOM predicted and radar measured power density time series are compared in Fig. 17 at the location 25.5118N, -79.8805W between April 2008 to May 2010. Predicted power densities by HYCOM-GOM exhibit a large RMSD (94%) and an order of magnitude higher bias difference than was observed for comparisons with the ADCP measurements near the surface 74% vs. 8.6%. This high bias is reflected in the comparison between predicted and measured mean, minimum and maximum values shown in Table 3. Nevertheless, HYCOM-GOM reproduces the measured power density pattern quite well.

Table 3. Performance metrics, HYCOM-GOM (28km x 28km) vs. HF Radar (30km x 30km) derived power density.

Time Interval	Power Density (W/m^2)						AR	Intcpt	R^2	RMSD (%)	Bias (%)
	Mean		Min		Max						
	Msrd	Pred	Msrd	Pred	Msrd	Pred					
Daily	1280	2220	69	439	3880	5160	0.62	1430	0.26	94	74

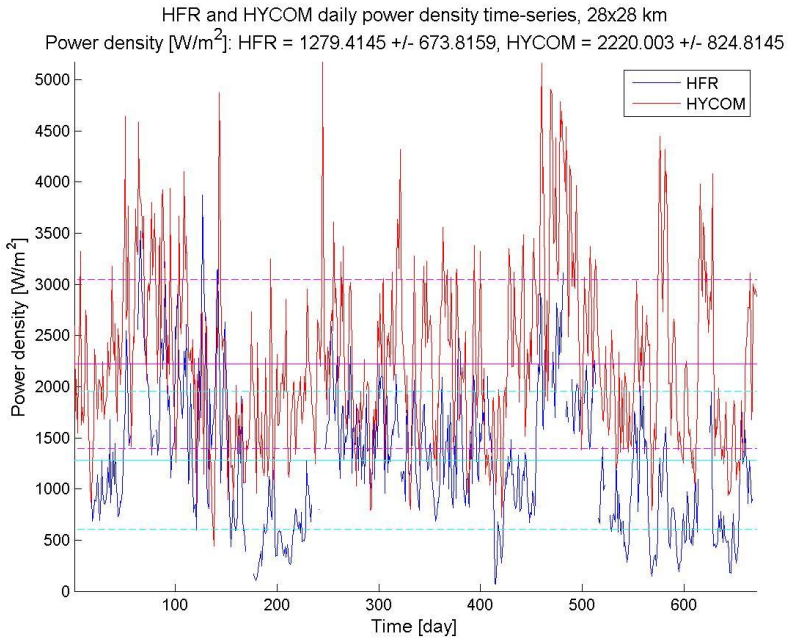

Figure 17. Comparison of power density time series derived from HYCOM-GOM simulations and HF radar data at 25.5118N, -79.8805W (April 2008 to May 2010).

Daily transport values derived from HYCOM-GOM and HF radar data are positively correlated, as shown in the scatter plot (Fig. 18), but exhibit large scatter about the line of perfect agreement and the best-fit line. The large scatter is reflected in the low correlation coefficient R^2=0.26. The data cloud is not centered on the best fit line, which corroborates with the large RMSD value and bias difference.

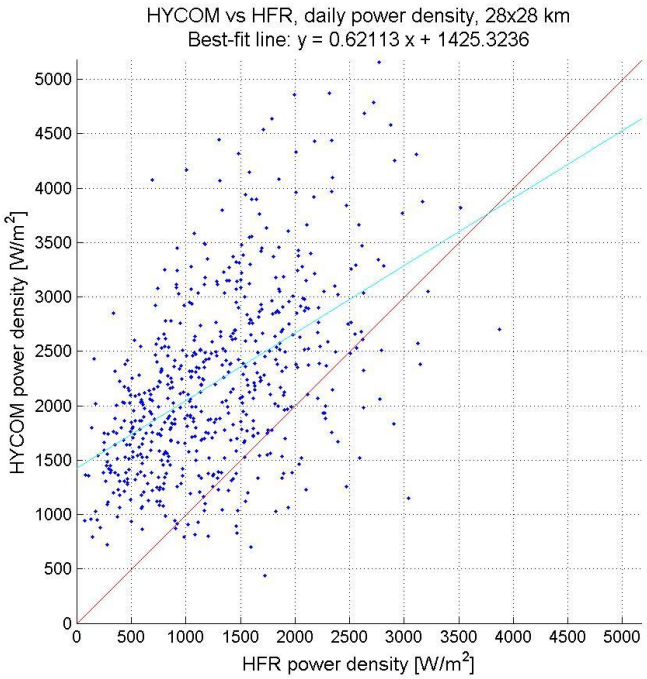

Figure 18. Comparison of power density time series derived from HYCOM-GOM simulations and HF radar data at 25.5118N, -79.8805W (April 2008 to May 2010).

HYCOM-GOM model performance is examined further by comparing plots of frequency histograms (Fig. 19), and cumulative frequency histograms (Fig. 20) of daily averaged power density derived by HYCOM-GOM and HF radar. Both predicted and measured daily averaged power density values are approximately the same shape, but the HYCOM histogram is shifted to the right, which indicates a clear systematic high bias. The shapes of the cumulative frequency histograms, shown in Fig. 20, also compare well, but, like the frequency histograms, show the pronounced high bias difference.

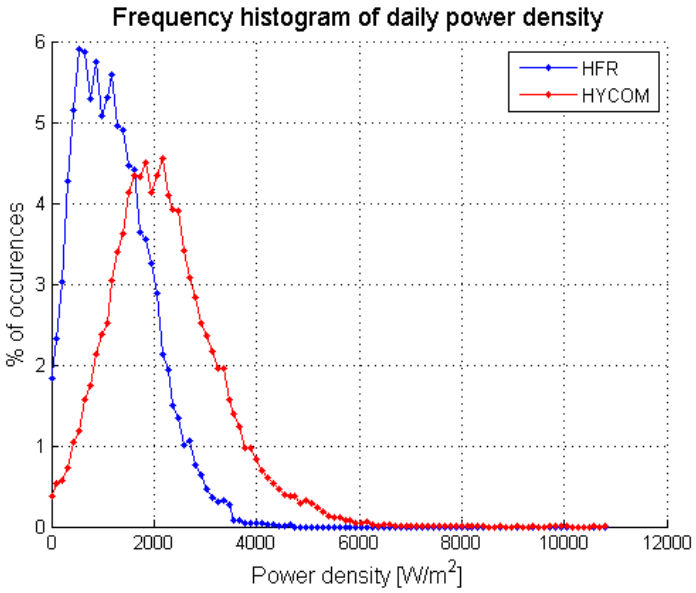

Figure 19. Comparison of frequency histograms of power density derived from HYCOM-GOM simulations and HF radar data.

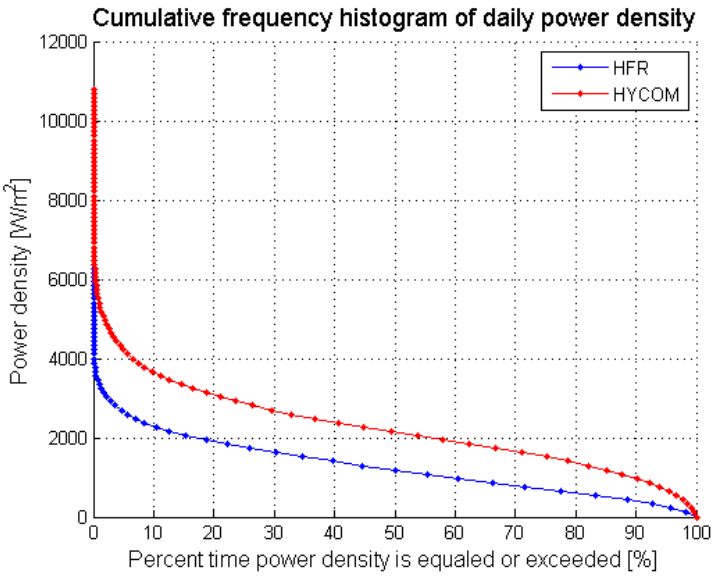

Figure 20. Comparison of cumulative frequency histograms of power density derived from HYCOM-GOM simulations and HF radar data.

CONCLUSIONS

This study examines the deviation of HYCOM-GOM outputs, including transport (flow), horizontal current, and power density, from outputs based on three independent observation sources to evaluate HYCOM-GOM performance. In addition, it compares the performance of the GLOBAL and GOM HYCOM models in predicting transport and vertical profiles of horizontal current and power density. The three independent data sources include NOAA's submarine cable data of transport, ADCP data at a high power density location, and HF radar data in the high power density region of the Florida Strait. Comparisons with these three independent observation sets, and HYCOM-GLOBAL outputs, indicate discrepancies with HYCOM model outputs, but overall that the HYCOM-GOM model can provide a *best-practical* assessment of the ocean current hydrokinetic resource in high power density regions like the Florida Strait. In particular, HYCOM-GOM predictions of the mean transport, and velocity and power density at the reference model depth of 60 m are in very good agreement with measurements. Although HYCOM-GOM performs less well at predicting the temporal variations of transport compared to HYCOM-GLOBAL for certain periods, this limitation should not adversely affect the accuracy of mean annual estimates of annual energy production. The significant underbias of HYCOM-GLOBAL predicted transport exhibits would, in comparison, lead to significant underprediction of mean annual energy production, and, therefore, a less desirable model than HYCOM-GOM for ocean current resource assessment. Further examination of the differences in data assimilation methodologies between HYCOM-GOM and HYCOM GLOBAL are warranted to explain the differences in performance between these models. Improvements to the HYCOM-GOM predicted temporal variations of transport might be improved by adopting the GLOBAL data assimilation methods when needed. Additional independent observational data, in particular stationary ADCP measurements, would be useful for expanding this model performance evaluation study. ADCP measurements are rare in ocean environments not influenced by tides, and limited to one location in the Florida Strait. HF radar data, although providing great spatial coverage, are limited to surface currents only.

ACKNOWLEDGEMENTS

The Office of Energy Efficiency and Renewable Energy (EERE) of the Department of Energy (DOE) provided funding for this review under DOE Contract DE-AC05-00OR22725. Figure 2 was developed by Xiufeng Yang, a post-doctoral research associate working under Kevin Haas at Georgia Tech. We thank those scientists involved with the collection, quality assurance and archiving of the independent observation sets used in this study. The Florida current cable and section data are made freely available on the Atlantic Oceanographic and Meteorological laboratory web page (http://www.aoml.noaa.gov/phod/floridacurrent/) and are funded by the NOAA Office of Climate Observations. The moored ADCP measurements were collected by the Southeast National Marine Renewable Energy Center (SEMREC) at Florida Atlantic University (FAU). The HF radar data was collected by the University of Miami and archived at Scripps Institution of Oceanography's Coastal Observing R&D Data Center. Alana Duerr, doctoral candidate at FAU, and Howard Hanson, professor of geosciences at FAU and chief scientist at the SEMREC provided information on the moored ADCP measurements. Scientists at Scripps, including Lisa Hazard and Paul Reuter, provided the HF radar data measurements; and Alison LaBonte, the Marine Hydrokinetic Technology Lead for DOE's water power program, and former Scripp's graduate, helped us acquire the HF radar data set. Nick Shay, professor of meteorology and physical oceanography at the University of Miami, as the principal investigator for the HF radar systems along the Florida coast.

REFERENCES

Baringer MO, Larsen JC (2001) Sixteen Years of Florida Current Transport at 27oN. J. of Geo. Res. 28 (16).

Baringer MO and Meinen CS, "Florida Current transport—Data access," DOC/NOAA/OAR/AOML: Atlantic Oceanogr. Meteorological Lab., 2010 [Online]. Available: http://www.aoml.noaa.gov/phod/floridacurrent/data_access.php

Barron CN, Smedstad LF, Dastugue JM, Smedstad OM (2007) Evaluation of ocean models using observed and simulated drifter trajectories: Impact of sea surface height on synthetic profiles for data assimilation. J. of Geo. Res. 112 (C07019). doi:10.1029/2006JC003982

Chapman RD, Shay LK, Graber HC, Edson JB, Karachintsev A, Trump CL, and Ross DB,(1997), On the accuracy of HF radar surface current measurements: Intercomparisons with ship-based sensors, J. Geophys. Res., 102(C8), 18,737– 18,748.

Defne Z, Haas KA, Fritz HM, Jiang L, Shi X, French SP, Smith BT, Neary VS and Stewart KM (Accepted February 2012) National geodatabase of tidal stream power resources in the USA. *Renewable and Sustainable Energy* Reviews.

Duerr AES., Dhanak M. (2012). An Assessment of the Hydrokinetic Energy Resource of the Florida Current. J. of Oceanic Eng., 37(2): TBD

Graber HC, Haus BK, Chapman RD, and Shay LK. (1997), HF radar comparisons with moored estimates of current speed and direction: Expected differences and implications, J. Geophys. Res., 102(C8), 18,749– 18,766.

Halliwell G, "HYCOM overview," 2002 [Online]. Available: http://www.hycom.org/attachments/067_overview.pdf

Hanson HP, Bozec A, and Duerr AES, "The Florida Current: A clean but challenging energy resource," *Eos Trans.*, vol. 92, no. 4, pp. 29–30, 2011.

Holbrook JR, and Frisch AS (1981), A comparison of near-surface CODAR and VACM measurements in the strait of Juan De Fuca, August 1978, J. Geophys. Res., 86(C11), 10,908–10,912.

Larsen JC (1991). Transport measurements from in-service undersea telephone cables, J. of Oceanic Eng., 16(4): 313-318.

Lawson, Michael. Personal communication, 14 June, 2012.

Matthews J P, Simpson JH, and Brown J (1988), Remote sensing of shelf sea currents using a high-frequency ocean surface current radar system, J. Geophys. Res., 93(C3), 2303– 2310.

Nadai A, Kuroiwa H, Mizutori M, and Sakai S (1997), Measurement of ocean surface currents by CRL HF ocean surface radar of the FMCW type. part 1. Radial current velocity, J. Oceanogr. Soc. Jpn., 53, 325– 342.

Meinen CS, Baringer MO, and Garcia RF, "Florida Current transport variability: An analysis of annual and longer-period signals," *Deep Sea Res. I, Oceanogr. Res. Papers*, vol. 57, no. 7, pp. 835–846, Jul. 2010.

Neary VS, Habib E, Fleming M (2004). "Hydrologic Modeling with NEXRAD Precipitation in Middle Tennessee." *Journal of Hydrologic Engineering*. 9(5), 1-11.

Parks AB, Shay LK, Johns WE, Martinez-Pedraja J, Gurgel KW (2009) HF radar observations of small scale surface current variability in Straits of Florida. J. of Geo. Res. 114 (C08002). doi:10.1029/2008JC005025

Raye R. "Characterization study of the Florida Current at 26.11 north latitude, 79.50 west longitude for ocean current power generation," M.S. thesis, Dept. Ocean Eng., Florida Atlantic Univ., Boca Raton, FL, 2002.

Reuter, Paul. Personal communication, 11 April, 2012.

Shay LK, Savidge D, Styles R, Seim H, and Weisberg RH (2008), High-frequency radar observing systems in SEACOOS, Mar. Technol. Soc. J., 42, 55–67.

Stewart KM, and Neary VS. "Validation of the Georgia Tech Regional tidal Current Resource Assessment Model and GIS Tool." ORNL/TM-2011/342.

VonArx, WS, Stewart HB, and Apel JR, "The Florida Current as a potential source of usable energy," in *Proc. Mac Arthur Workshop Feasibility of Extracting Usable Energy From the Florida Current*, 1974, pp. 91–101.

Yoshikawa Y, Masuda A, Marubayashi K, Ishibashi M, and Okuno A (2006). "On the accuracy of HF radar measurement in the Tsushima Strait," J. Geophys. Res., 111, C04009, doi:10.1029/2005JC003232.